Temperature dependence and fragmentation of the particle-hole giant resonances

E. C. Seva and H. M. Sofia
Departamento de Física, Comisión Nacional de Energía Atómica and CONICET, Avenida del Libertador 8250, 1429 Buenos Aires, Argentina
(Received 4 June 1997)

We evaluate the spreading width of the giant multipole resonances at finite temperature using the discontinuity in the second derivative of the Green's function of the vibrational boson, in the Matsubara's framework. Our method allows us to identify the processes that contribute to the spreading width in terms of the Feynman diagrammatic expansion of the full boson propagator. We have applied the calculation of the spreading width to the ^{208}Pb and the ^{90}Zr obtaining an increment of the spreading width with the temperature. We have not reached any saturation of the spreading width increment, at least up to the temperature of our calculation. [S0556-2813(97)03912-5]

PACS number(s): 24.30.Cz, 21.60.Jz

I. INTRODUCTION

Properties of the nuclei at very high temperature can be obtained through experiments that measured γ rays, emitted during the decay, in particular from the energy region of the giant dipole resonances (GDR) [1]. It is also possible to measure the properties of nuclei at very high excitation energies using heavy ion collisions [2]. Recent experimental data on the GDR in very hot nuclei and their thermal fluctuations have been reported in the Gröningen Conference on Giant Resonances [3–6].

At high excitation energies the nuclear level density increases so rapidly that it is practically impossible to study transitions between individual levels and therefore a statistical description of the system becomes adequate. The usual way to follow in this case is to replace the compound systems, with definite excitation energy and definite particle number, by the grand canonical ensemble of the nuclei.

Several approaches to the thermodynamical properties of finite systems have been developed. They are usually based on a thermal variational description of the systems that yields the temperature Hartree-Fock-Bogoliubov (TDHFB) [7–9] equations as the mean-field approximation.

In past years, there have been developed several studies of the behavior of nuclei at finite temperature. In particular the behavior of the energy centroid, width, structure, and strength of the giant multipole resonances (GMR), is attracting the attention of the nuclear physicists [10–12].

Experimental analysis of the damping of the giant resonances shows that the total width of the GDR increases strongly [13] at moderate temperature ($\sim T^3$) with the possibility of saturation at high temperatures, a problem that is still a controversial point [14–16]. All theoretical studies give no clear explanation of the observed increment. Thermal fluctuations of the nuclear shape have been proposed [17] but they give an increment of the width that goes approximately as $T^{1/2}$. Moreover, when thermal fluctuations are treated dynamically, it has been shown that a motion-narrowing process arises. This process inhibits the previous result for temperature above $T=1$ MeV and strongly weakens the temperature dependence of the width [18,19]. Another effect comes from the angular momentum transferred to the compound nucleus that induces a deformation of the nucleus, producing a fast rotational motion. In Ref. [20] it is shown that angular momentum effects are responsible for most of the observed increase of the GDR width. However, it is not enough to explain the data, especially at low temperatures and little deformations, and at high temperatures, where the effects are constrained by the maximum angular momentum possible without producing nuclear fission. The latter one makes it possible to separate temperature effects from angular momentum effects, giving a better insight of the different thermal phenomena that could contribute to the broadening of the giant resonance.

In this paper we start considering that the centroid of the distribution of the giant multipole strength can be described as a particle-hole excitation built on a highly excited ground state, through a temperature dependent random phase approximation (TRPA) [21].

The damping of the giant resonance collective excitations is considered to proceed through different decaying processes.

(a) The ''escaping width'' is related to direct particle emission and is associated with the portion of the GMR having the particle (of the particle-hole excitation) in the continuum [22–25].

(b) The ''Landau damping'' appeared at the level of mean field theory and expressed the fragmentation of the multipole strength in different roots of the RPA at energies near the GMR energy. It has been studied [26] and seems to be neither an important damping process nor one that varies too much with temperature.

(c) The ''spreading width'' provides a direct measurement of the fragmentation of GMR into neighboring more complicated configurations, mainly two-particle–two-hole excitations. This width is directly related to the electromagnetic damping of the GMR and is influenced by variations in the temperature. At zero temperature considerable work has been developed on this subject [27–31], but at finite temperature there are only few approaches that disagree in some of their results [32,33], and more recently [12]. The spreading width at finite temperature is also the main purpose of our work.

In this article we develop a method to calculate the dependence of the spreading width on the temperature, which is a logical extension of our previous work (see Ref. [34]). In that paper we studied the time evolution of the collective

degrees of freedom, which leads to a simple diagrammatic expansion of the second moment of the strength distribution (directly related to the spreading width σ). In our work we utilize temperature (instead of time) dependent Green's Functions, based on the Matsubara finite temperature formalism. A real-time Green's function can be found by analytic continuation of the frequency variable. In the Matsubara formalism we can evaluate consistently the self-energy to a desired order of perturbation theory in the grand canonical ensemble. The main advantage of this type of description is that the processes taken into account are specified and therefore the approximation made is more clearly understood from a physical point of view.

Our formalism, even if related to the perturbative expansion of the nuclear field theory (NFT) [35,36], works on a complete system of collective states. In this sense it is different from Ref. [32] where they prefer to work with a mixture of boson (TRPA roots) and particle-hole overcomplete basis. The price we have to pay is to calculate all the roots of the TRPA in order to have the complete basis. The advantage we obtain is that the number of diagrams needed to calculate all the contributions to the leading order are highly reduced. In this way we define a one-boson two-boson effective interaction vertex that allows the calculation of the spreading width exactly up to the first order in the NFT expansion.

The article is organized in the following way. In Sec. II we make a review of some properties that can be obtained from the short time behavior of the collective-state Green's functions and extent it to finite temperature. In Sec. III we develop the formalism diagrammatically in order to show the contributions that are considered within our method. In Sec. IV we work out a temperature dependent vertex of interaction between one and two TRPA bosons. The spreading width is related to the sum of the square of these vertices times some expression depending on the temperature occupation probabilities for the bosons. We will show that the vertices themselves depend on the fermionic temperature occupation-probabilities. In Sec. VI we applied our formalism to the giant dipole resonance of the ^{90}Zr and ^{208}Pb using an isoscalar-isovector separable interaction.

II. STATEMENT OF THE FORMALISM

The relation between the short time behavior of the Green's functions and different properties of the nuclear systems has been analyzed in Ref. [37]. In a previous paper, we have used the above properties to isolate the Feynman diagrams that contribute to the spreading width of the particle-hole giant resonances [34]. Following the same idea we generalized the method used for the calculation of the spreading width at zero temperature, to finite temperature. Therefore, we follow the Matsubara formalism that simplifies greatly the description of finite temperature systems using temperature dependent Green's function (TDGF).

The TDGF does not dependent on time as the usual Green's function does, but on a fictitious imaginary variable $\tau = it$ defined in the interval 0 to $1/k_B T$ (where T is the temperature of the system and k_B is the Boltzman constant). We do not calculate the thermodynamical quantities but instead we evaluate the TDGF, using the perturbative expansion described by the corresponding Feynman-Goldstone diagrams [38–40]. The main difference from the treatment at zero temperature is that, instead of integrating the time from $-\infty$ to ∞ in each vertex, the variable τ is integrated from 0 to $1/k_B T$. In the future we will call $\beta = 1/k_B T$.

We start defining a Hamiltonian that can be split into a one-boson Hamiltonian H_0 and a residual interaction H_1.

$$H_0 = H_{\mathrm{TRPA}} + h, \quad H_1 = V - h \tag{2.1}$$

where H_{TRPA} is the one TRPA boson Hamiltonian while h is an arbitrary one-boson potential that contains all the residual interactions or Pauli corrections that can mix the different root of the TRPA. V is the rest of the interaction of a general two-body force. We will start from the TRPA boson representation $|n\rangle$ that diagonalizes H_0.

The one-boson temperature dependent Green's function, corresponding to the total Hamiltonian in the Lehmann representation, is given by the following equation:

$$\begin{aligned} G_{n,n'}(\tau) &= \mathrm{Tr}[e^{\beta(\Omega - H + \mu N)}\{\Gamma_n(\tau)\Gamma^{\dagger}_{n'}(0)\,\theta(\tau) + \Gamma^{\dagger}_{n'}(0)\Gamma_n(\tau)\,\theta(-\tau)\}] \\ &= \frac{\mathrm{Tr}[e^{-\beta(H-\mu N)}\{\Gamma_n(\tau)\Gamma^{\dagger}_{n'}(0)\,\theta(\tau) + \Gamma^{\dagger}_{n'}(0)\Gamma_n(\tau)\,\theta(-\tau)\}]}{Tr[e^{-\beta(H-\mu N)}]}. \end{aligned} \tag{2.2}$$

The quantity Ω in the exponential is the thermodynamical potential, μ is the chemical potential, N the particles-number operator, H the total Hamiltonian, and $\Gamma^{\dagger}_n$ creates a TRPA boson with energy ω_n.

We can expand the temperature dependent Green's function (see Fig. 1) in Feynman diagrams generated by the Dyson's equation:

$$G_{n,n'}(\tau'' - \tau') = G^0_n(\tau'' - \tau')\,\delta_{n,n'} + \int\int d\tau_1 d\tau_2 \sum_m G^0_n(\tau_1 - \tau') F_{n,m}(\tau_2 - \tau_1) G_{m,n'}(\tau'' - \tau_2), \tag{2.3}$$

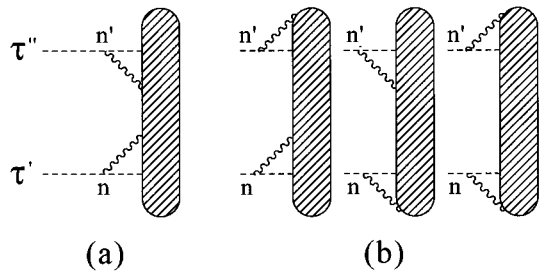

FIG. 1. General form of the Feynman-Goldstone diagrams contributing to the one-boson Green's function. The blobs could be anything while they are connected. (a) Schematic representation of restricted diagrams. (b) The same for unrestricted diagrams.

where $F_{n,m}(\tau_2-\tau_1)$ is the self-energy of the problem and is represented by the same diagrams of the Fig. 1 without the external lines. $G^0_n(\tau)$ is the bare TRPA boson Green's function. The relevant diagrams here are depending on τ instead of the normal ones that depend on the energy. In the blob there could be anything including the vertices of the Hamiltonian that introduce the ground state fluctuations.

In Ref. [37], it is shown that a lot of relevant information, including the spreading width of the GMR, can be obtained from the short time behavior of the Green's function and its derivative (around $t_2-t_1=0$). In our case we extend the method to short-τ behavior of TDGF:

$$\frac{^n}{\partial\tau^n}G_{n,n'}(\tau)\bigg|_{\tau\to 0+} - \frac{\partial^n}{\partial\tau^n}G_{n,n'}(\tau)\bigg|_{\tau\to 0-}. \qquad (2.4)$$

Following Ref. [37], we classified the Feynman diagrams in two types. (a) Restricted diagrams [Fig. 1(a)]. These are the diagrams that have a continuous chain of boson and fermion lines, where the τ intermediate are always between τ' and τ'', i.e.,

$$\tau' < \tau_1 < \tau_2 < \cdots < \tau''$$

or

$$\tau' > \tau_1 > \tau_2 > \cdots > \tau'.$$

(b) Unrestricted diagrams [Fig. 1(b)]. In these diagrams, the intermediate τ's do not follow the above rules. Therefore, all such diagrams are continuous when $\tau''\to\tau'$, and do not contribute to the discontinuity at $\tau''=\tau'$.

The restricted diagrams, instead, exist only for $\tau'>\tau''$ or $\tau'<\tau''$ with a chain of intermediate states between them. If the diagram contains more than one link, each integration produces a factor $\tau'-\tau''$ when $\tau'\to\tau''$. Therefore, the contribution to the discontinuity of the nth derivative is given only by the restricted diagrams that have a maximum of n intermediate vertices.

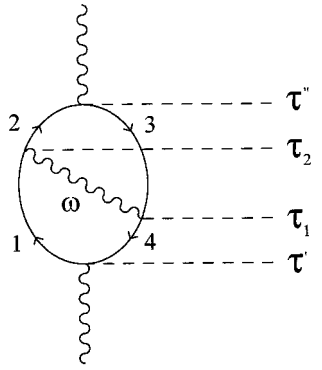

FIG. 2. One of the lowest order correction to the vibrational temperature dependent Green's function. An arrowed line describes the particle propagation while a wavy line describes the vibrational boson.

In Ref. [34], we have showed that the second moment of the strength distribution is related to the second derivative of the Green's function. Here we extend the formalism to TDGF:

$$\langle n|H^2|n\rangle = \Big(\lim_{\tau''-\tau'\to 0+} - \lim_{\tau''-\tau'\to 0-}\Big)\frac{\partial^2}{\partial\tau''\partial\tau'}G(n,n;\tau''-\tau')$$

$$= \sum_m W_m^2\langle\Psi_0|\Gamma_n|\psi_m\rangle\langle\psi_m|\Gamma_n^+|\Psi_0\rangle$$

$$- \sum_m W_m^2\langle\Psi_0|\Gamma_n^+|\psi_{\overline{m}}\rangle\langle\psi_{\overline{m}}|\Gamma_n|\Psi_0\rangle. \qquad (2.5)$$

The diagrams that contribute to the short-time second derivative have no more than two interaction vertices. If we subtract the ones contributing to the $(\langle n|H|n\rangle)^2$ the only diagrams that remain are restricted diagrams, which begin and end with an interaction vertex and have no intermediate state equal to the initial one [34]. It must be noted that in the limit $\tau''-\tau'=0$, the two vertices occur at the same parameter τ and the propagator between them disappears, giving a contribution equal to the product of the two matrix elements.

The main difference with the zero temperature case [34] is the fact that the fermions and bosons have a temperature occupation probability different from zero. Therefore, the hole and particle type of levels are washed up and all of them contribute to the diagrams with some probability of being occupied (holes) or unoccupied (particles). Besides, in this case, it is not possible to neglect the negative TRPA roots anymore, because both of them contribute to the diagrams, depending on the temperature occupation probability of the boson.

III. SELF-ENERGY CORRECTION TO THE TDGF

In this section we will show the more important features of the lowest corrections to the unperturbed TDGF. We calculate in detail, as an example, the self-energy of one simple diagram (see Fig. 2)

$$F(\tau''-\tau')=\frac{1}{\beta^5}\sum_{1,2,3,4,\lambda}\mathcal{V}(J_1,J_2;\lambda)\mathcal{V}(J_3,J_4;\lambda)\mathcal{V}(J_2,J_3;GR)\mathcal{V}(J_1,J_4;GR)$$
$$\times\sum_{p_{n_1},p_{n_2},p_{n_3},p_{n_4}}\sum_{k_n}\int d\tau_1 d\tau_2\frac{e^{-ip_{n_1}(\tau_2-\tau')}}{ip_1-\tilde{\varepsilon}_1}\frac{e^{-ip_{n_2}(\tau''-\tau_2)}}{ip_{n_2}-\tilde{\varepsilon}_2}\frac{e^{-ip_{n_3}(\tau_1-\tau'')}}{ip_{n_3}-\tilde{\varepsilon}_3}\frac{e^{-ip_{n_4}(\tau'-\tau_1)}}{ip_{n_4}-\tilde{\varepsilon}_4}$$
$$\times\left(\frac{1}{ik_n-\omega_\lambda}-\frac{1}{ik_n+\omega_\lambda}\right)e^{-ik_n(\tau_2-\tau_1)}, \tag{3.1}$$

where i labels a particle state with energy $\tilde{\epsilon}_i=\epsilon_i-\mu$, λ labels a TRPA vibration with energy ω_λ, $\mathcal{V}(1,2;\lambda)$ is the particle-vibration coupling strength, $p_{n_i}=(2n_i+1)\pi/\hbar\beta$, $k_n=2n\pi/\hbar\beta$ are the imaginary Fourier transform frequencies of fermions and bosons, n_i,n are integers, and the temperature dependence is in the β factor. The two terms present in the intermediate state of the boson reflect the fact that it is necessary to include, on an equal footing, the negative-energy TRPA roots. After performing the integration on the intermediate τ, making the sum on the imaginary frequencies and doing some algebraic rearrangements, we arrive at

$$F(\tau''-\tau')=\frac{1}{\beta}\sum_{k_n=par}\frac{e^{-ik_n(\tau''-\tau')}}{2}\sum_{J_1,J_2,J_3,J_4,\lambda}\mathcal{V}(J_1,J_2;\lambda)\mathcal{V}(J_3,J_4;\lambda)\mathcal{V}(J_2,J_3;GR)\mathcal{V}(J_1,J_4;GR)$$
$$\times\left\{\frac{[(1-n_{J_1})(1+n_\omega)+n_{J_1}n_\omega](2n_{J_2}-1)}{(ik_n+\tilde{\varepsilon}_{41})(-ik_n+\tilde{\varepsilon}_{23})(\tilde{\varepsilon}_{21}-\omega_\lambda)}+\frac{[(1-n_{J_1})(1+n_\omega)+n_{J_1}n_\omega](2n_{J_3}-1)}{(ik_n+\tilde{\varepsilon}_{41})(ik_n+\tilde{\varepsilon}_{32})(ik_n+\tilde{\varepsilon}_{31}-\omega_\lambda)}\right.$$
$$-\frac{[n_{J_1}n_\omega-(1-n_{J_1})(1+n_\omega)]}{(ik_n+\tilde{\varepsilon}_{41})(\tilde{\varepsilon}_{12}+\omega_\lambda)(ik_n-\tilde{\varepsilon}_{13}-\omega_\lambda)}-\frac{[(1-n_{J_4})(1+n_\omega)+n_{J_4}n_\omega](2n_{J_2}-1)}{(ik_n+\tilde{\varepsilon}_{41})(ik_n-\tilde{\varepsilon}_{23})(ik_n-\tilde{\varepsilon}_{24}+\omega_\lambda)}$$
$$\left.-\frac{[(1-n_{J_4})(1+n_\omega)+n_{J_4}n_\omega](2n_{J_3}-1)}{(ik_n+\tilde{\varepsilon}_{41})(ik_n+\tilde{\varepsilon}_{32})(\tilde{\varepsilon}_{34}-\omega_\lambda)}-\frac{[n_{J_4}n_\omega-(1-n_{J_4})(1+n_\omega)]}{(ik_n+\tilde{\varepsilon}_{41})(ik_n+\tilde{\varepsilon}_{42}+\omega_\lambda)(\tilde{\varepsilon}_{43}+\omega_\lambda)}\right\}$$
$$-\{\text{same as above with } \omega_\lambda\rightarrow-\omega_\lambda\}, \tag{3.2}$$

where $\tilde{\varepsilon}_{ij}=\tilde{\varepsilon}_i-\tilde{\varepsilon}_j$ and $n_\omega=(e^{\beta\omega_\lambda}-1)^{-1}$, $n_{J_i}=(e^{\beta\tilde{\varepsilon}_i}+1)^{-1}$ are the Bose and Fermi temperature occupation probability. Note that the appearance of Bose occupation factors is a consequence of treating all the particle-hole vibrations as quasibosons, as it is assumed in the TRPA approximation.

This expression can be developed in such a way that each time permutation diagram can be clearly identified. Therefore, we will rebuild the self-energy [Eq. (3.2)], corresponding to the Fig. 2, in order to analyze the different τ permutation and consider the two solutions of the TRPA ($\pm\omega_\lambda$). Performing some algebraic calculation, we obtain

$$F(\tau''-\tau')=\frac{1}{\beta}\sum_{k_n=par}e^{-ik_n(\tau''-\tau')}\sum_{J_1,J_2,J_3,J_4,\lambda}\mathcal{V}(J_1,J_2;\lambda)\mathcal{V}(J_3,J_4;\lambda)\mathcal{V}(J_2,J_3;GR)\mathcal{V}(J_1,J_4;GR)$$
$$\times\left\{\frac{[(1-n_{J_1})(1-n_{J_2})n_{J_3}n_{J_4}(1+n_\omega)-n_{J_1}n_{J_2}(1-n_{J_3})(1-n_{J_4})n_\omega]}{(ik_n+\tilde{\varepsilon}_{41})(ik_n-\tilde{\varepsilon}_{23})(ik_n-\tilde{\varepsilon}_{13}-\omega_\lambda)}\right.$$
$$+\frac{[(1-n_{J_1})(1-n_{J_2})n_{J_3}(1-n_{J_4})(1+n_\omega)-n_{J_1}n_{J_2}(1-n_{J_3})n_{J_4}n_\omega]}{(ik_n-\tilde{\varepsilon}_{13}-\omega_\lambda)(ik_n-\tilde{\varepsilon}_{23})(\tilde{\varepsilon}_{43}+\omega_\lambda)}$$
$$+\frac{[(1-n_{J_1})n_{J_2}n_{J_3}n_{J_4}(1+n_\omega)-n_{J_1}(1-n_{J_2})(1-n_{J_3})(1-n_{J_4})n_\omega]}{(ik_n-\tilde{\varepsilon}_{14})(ik_n-\tilde{\varepsilon}_{13}-\omega_\lambda)(\tilde{\varepsilon}_{12}+\omega_\lambda)}$$
$$\left.+\frac{[n_{J_1}(1-n_{J_2})n_{J_3}n_{J_4}n_\omega-(1-n_{J_1})n_{J_2}(1-n_{J_3})(1-n_{J_4})(1+n_\omega)]}{(ik_n-\tilde{\varepsilon}_{23})(ik_n-\tilde{\varepsilon}_{24}+\omega_\lambda)(\tilde{\varepsilon}_{21}-\omega_\lambda)}\right.$$

$$
\begin{aligned}
&+\frac{[(1-n_{J_1})(1-n_{J_2})(1-n_{J_3})n_{J_4}n_\omega - n_{J_1}n_{J_2}n_{J_3}(1-n_{J_4})(1+n_\omega)]}{(ik_n-\tilde{\varepsilon}_{14})(ik_n-\tilde{\varepsilon}_{24}+\omega_\lambda)(\tilde{\varepsilon}_{34}-\omega_\lambda)}\\
&+\frac{[(1-n_{J_1})(1-n_{J_2})n_{J_3}n_{J_4}n_\omega - n_{J_1}n_{J_2}(1-n_{J_3})(1-n_{J_4})(1+n_\omega)]}{(ik_n-\tilde{\varepsilon}_{14})(ik_n-\tilde{\varepsilon}_{24}+\omega_\lambda)(ik_n-\tilde{\varepsilon}_{23})}\\
&+\frac{[n_{J_1}(1-n_{J_2})n_{J_3}(1-n_{J_4})(1+n_\omega)-(1-n_{J_1})n_{J_2}(1-n_{J_3})n_{J_4}n_\omega]}{(\tilde{\varepsilon}_{14}-\tilde{\varepsilon}_{23})(\tilde{\varepsilon}_{43}+\omega_\lambda)(ik_n-\tilde{\varepsilon}_{14})}\\
&+\frac{[n_{J_1}(1-n_{J_2})n_{J_3}(1-n_{J_4})(1+n_\omega)-(1-n_{J_1})n_{J_2}(1-n_{J_3})n_{J_4}n_\omega]}{(\tilde{\varepsilon}_{14}-\tilde{\varepsilon}_{23})(\tilde{\varepsilon}_{43}+\omega_\lambda)(-ik_n+\tilde{\varepsilon}_{23})}\\
&+\frac{[(1-n_{J_1})n_{J_2}n_{J_3}(1-n_{J_4})(1+n_\omega)-n_{J_1}(1-n_{J_2})(1-n_{J_3})n_{J_4}n_\omega]}{(\tilde{\varepsilon}_{43}+\omega_\lambda)(\tilde{\varepsilon}_{12}+\omega_\lambda)(ik_n-\tilde{\varepsilon}_{13}-\omega_\lambda)}\\
&+\frac{[(1-n_{J_1})n_{J_2}n_{J_3}(1-n_{J_4})(1+n_\omega)-n_{J_1}(1-n_{J_2})(1-n_{J_3})n_{J_4}n_\omega]}{(\tilde{\varepsilon}_{43}+\omega_\lambda)(\tilde{\varepsilon}_{12}+\omega_\lambda)(-ik_n-\tilde{\varepsilon}_{42}-\omega_\lambda)}\\
&+\frac{[(1-n_{J_1})n_{J_2}(1-n_{J_3})n_{J_4}(1+n_\omega)-n_{J_1}(1-n_{J_2})n_{J_3}(1-n_{J_4})n_\omega]}{(\tilde{\varepsilon}_{23}+\tilde{\varepsilon}_{41})(\tilde{\varepsilon}_{21}-\omega_\lambda)(ik_n-\tilde{\varepsilon}_{14})}\\
&+\left.\frac{[(1-n_{J_1})n_{J_2}(1-n_{J_3})n_{J_4}(1+n_\omega)-n_{J_1}(1-n_{J_2})n_{J_3}(1-n_{J_4})n_\omega]}{(\tilde{\varepsilon}_{23}+\tilde{\varepsilon}_{41})(\tilde{\varepsilon}_{21}-\omega_\lambda)(-ik_n+\tilde{\varepsilon}_{23})}\right\}\\
&-\{\text{same as above with } \omega_\lambda\rightarrow-\omega_\lambda\}. \qquad (3.3)
\end{aligned}
$$

Each term of the above equation could be associated with a diagram that represents a τ permutation of the original one. It can be observed that the calculation of each term follows well-defined rules.

The numerator of each term takes into account the Bose and Fermi temperature occupation numbers and is easily constructed looking at the circulation of the diagram (for each τ permutation). The particles that appear in the diagram contribute with $(1-n_J)$ factors, while the holes contribute with n_J factors. On the other hand, the bosons with positive roots of the TRPA $(+\omega_\lambda)$ contribute with $(1+n_\omega)$ factors and are represented by wavy lines with upward arrows, while the negative roots $(-\omega_\lambda)$ contribute with n_ω factors, being represented by a wavy line with downward arrows.

For each term another always exists with the same denominator that can be constructed changing the direction of all the arrows and consequently the temperature occupation numbers, namely changing $[(1-n_J)\leftrightarrow n_J,(1+n_\omega)\leftrightarrow n_\omega]$. This new diagram represents the permutation of $\tau'\leftrightarrow\tau''$ (see Fig. 2). The sign between these two terms depends on a phase $(-)^A$, where A is the number of intermediate states in the diagram. The denominators follow the usual rules used in the NFT or Raileigh-Schrödinger perturbation theory. They can be written as a product of the energy difference between the initial state and the intermediate states.

As an example, the second term of Eq. (3.3) represents the τ permutation of Fig. 3 and one can easily obtain its contribution following the previous rules.

In Ref. [32] the spreading width of the GMR is calculated using the diagram of Fig. 2, but considering only two temporal permutations, the terms 1 and 6 of Eq. (3.3), and the interchange of $\omega_\lambda\rightarrow-\omega_\lambda$. They neglect the other temporal permutations assuming that they are only important if the vibrational state are strongly collective. Besides, they work with the fermion-occupation numbers at zero temperature, neglecting the variation produced on these numbers by the increasing temperature. This assumption implies neglecting the new configurations of particle-particle and hole-hole that arise at finite temperature. They use, instead of the Eq. (3.3), the following one:

$$(1-n_{J_1}),(1-n_{J_2}),n_{J_3},n_{J_4}\rightarrow 1, \qquad (3.4)$$

producing

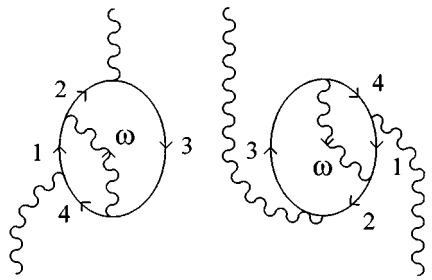

FIG. 3. τ permutations of the diagram of Fig. 2. The two diagrams have the same denominator but all the thermal occupation numbers are changed from particle to hole and vice versa. An intermediate wavy line, with an upward arrow, represents a positive TRPA root while a downward arrow is a negative TRPA root.

$$F(\tau''-\tau')=\frac{1}{\beta}\sum_{k_n=par} e^{-ik_n(\tau''-\tau')}\sum_{J_1,J_2,J_3,J_4,\lambda}\mathcal{V}(J_1,J_2;\lambda)\mathcal{V}(J_3,J_4;\lambda)\mathcal{V}(J_2,J_3;GR)\mathcal{V}(J_1,J_4;GR)$$
$$\times\left\{\frac{(1+n_\omega)}{(ik_n+\tilde{\varepsilon}_{41})(ik_n-\tilde{\varepsilon}_{23})(ik_n-\tilde{\varepsilon}_{13}-\omega_\lambda)}+\frac{n_\omega}{(ik_n-\tilde{\varepsilon}_{14})(ik_n-\tilde{\varepsilon}_{24}+\omega_\lambda)(ik_n-\tilde{\varepsilon}_{23})}\right.$$
$$\left.+\frac{n_\omega}{(ik_n+\tilde{\varepsilon}_{41})(ik_n-\tilde{\varepsilon}_{23})(ik_n-\tilde{\varepsilon}_{13}+\omega_\lambda)}+\frac{(1+n_\omega)}{(ik_n-\tilde{\varepsilon}_{14})(ik_n-\tilde{\varepsilon}_{24}-\omega_\lambda)(ik_n-\tilde{\varepsilon}_{23})}\right\}, \quad (3.5)$$

that is, Eq. (17) of Ref. [32].

IV. SPREADING WIDTH OF THE GMR

The spreading width of the GMR at finite temperature depends on the discontinuity of the second derivative of the Green's function [see Eq. (2.5)]. The diagrams that contribute to the width [34] are those that begin and end with an interaction and have no intermediate state equal to the initial one. The relevant diagrams are some of the different τ permutations of the diagrams shown in Fig. 4. In the NFT framework, these diagrams contribute to the leading order correction of the energy of the one boson state.

However, different from the NFT that works with an overcomplete basis of RPA bosons and particle holes, we prefer to work within a complete basis. In this case, the TRPA vertices are not considered interaction vertices but only the amplitude of the fermionic pair in the collective state. The only interaction vertices considered are those changing the number of bosons (or particle-hole pair) by ± 1 [34]. In this way the number of diagrams involved are reduced drastically. On the other hand, the price we have to pay in order to work in a complete collective basis is to use as intermediate states all the TRPA roots.

The calculation cannot be made in the same way as has been done at zero temperature [34], because the Bose and Fermi temperature occupation numbers are present in the sum of the different contributions. Therefore, we developed a method to sum the diagrams that can be applied to the calculation of the spreading width at finite temperature. In Appendix A, we show how the Bose and Fermi occupation numbers can be factorized summing conveniently the contributions to σ^2.

From the above explanation we see that the relevant diagrams contributing to σ^2 are those restricted diagrams that have two interactions changing the number of bosons (or particle-hole pair) by ± 1, linked to the initial or final boson line. These vertices must act between the annihilation of the initial boson and the creation of the final one.

We observe, within our method, that the contribution of the relevant diagrams to the discontinuity of the second derivative of the temperature boson Green's function (see Appendix A) is reduced to the square of the matrix element between one-boson and two-boson state. The main difference with the zero temperature case is that these matrix elements depend on the Fermi occupation numbers only, while the Bose occupation numbers appear in the definition of σ^2 because of the temperature-dependent two-boson propagator.

The final conclusion is that the only intermediate states that can be reached from the one-boson state, through the two-body interaction in leading order in perturbation theory, are the two-boson states shown diagrammatically in Fig. 5. Those of Fig. 5(a) are the forward matrix element between

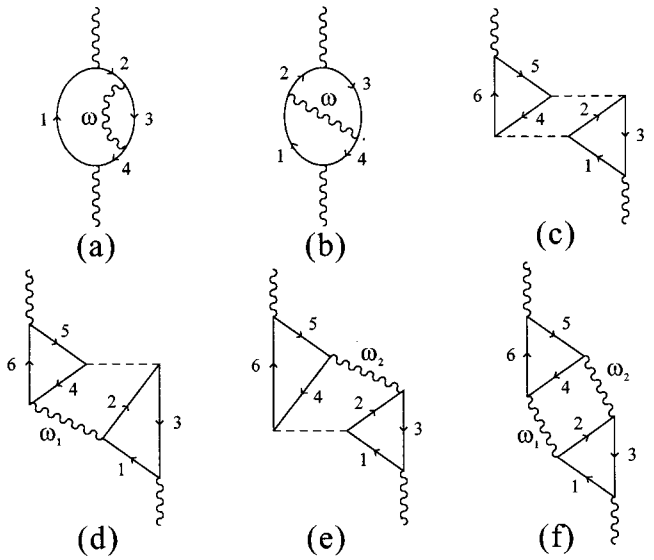

FIG. 4. The leading-order correction to the energy of the one-boson state. All the τ permutations (that are not in the figure) contribute to the spreading width and must be included in the calculation.

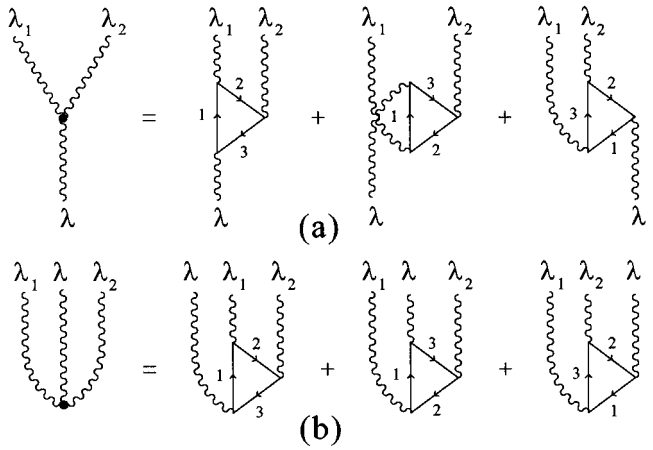

FIG. 5. Two-body matrix elements (including direct and exchange parts) that contribute to the one-boson two-bosons effective interaction vertex. (a) Diagrammatic representation of the forward vertex Eq. (4.1) and (b) of the backward vertex Eq. (4.2).

one and two-boson states, while those of Fig. 5(b) are related to the backward vertex of the TRPA and show the dependence with the ground state fluctuations. It must be noted that these diagrams are temperature dependent, so both forward and backward vertices, have the possibility that the two-boson states have positive (negative) energies, i.e., propagate in the positive (negative) direction of τ.

The vertices of Fig. 5 are

$$\langle \lambda n|\mathcal{H}|\lambda_1 n_1,\lambda_2 n_2\rangle = \sum_{J_1,J_2,J_3} \{[X^{(n_1)}_{J_1J_2}(\lambda_1)X^{(n)}_{J_1J_3}(\lambda)+Y^{(n_1)}_{J_1J_2}(\lambda_1)Y^{(n)}_{J_1J_3}(\lambda)]\Lambda^{(n_2)}_{J_2J_3}(\lambda_2)[(1-n_{J_1})n_{J_2}n_{J_3}-n_{J_1}(1-n_{J_2})(1-n_{J_3})]$$
$$+X^{(n_2)}_{J_2J_3}(\lambda_2)Y^{(n_1)}_{J_1J_3}(\lambda_1)\Lambda^{(n)}_{J_1J_2}(\lambda)[n_{J_1}n_{J_2}(1-n_{J_3})-(1-n_{J_1})(1-n_{J_2})n_{J_3}]\}$$
$$\times\sqrt{2\lambda_1+1}\sqrt{2\lambda_2+1}(-)^{J_1+J_3+\lambda_2+\lambda}\begin{Bmatrix}\lambda & \lambda_1 & \lambda_2\\ J_3 & J_2 & J_1\end{Bmatrix}\sqrt{1+\delta_{n_1n_2}} \tag{4.1}$$

and

$$\langle 0|\mathcal{H}|[\lambda_1 n_1,\lambda_2 n_2]_\lambda,\lambda n\rangle \sum_{J_1,J_2,J_3} \{[X^{(n_1)}_{J_1J_2}(\lambda_1)Y^{(n)}_{J_1J_3}(\lambda)+X^{(n)}_{J_1J_3}(\lambda)Y^{(n_1)}_{J_1J_2}(\lambda_1)]\Lambda^{(n_2)}_{J_2J_3}(\lambda_2)[(1-n_{J_1})n_{J_2}n_{J_3}-n_{J_1}(1-n_{J_2})(1-n_{J_3})]$$
$$+Y^{(n_2)}_{J_2J_3}(\lambda_2)X^{(n_1)}_{J_1J_3}(\lambda_1)\Lambda^{(n)}_{J_1J_2}(\lambda)[n_{J_1}n_{J_2}(1-n_{J_3})-(1-n_{J_1})(1-n_{J_2})n_{J_3}]\}\sqrt{2\lambda_1+1}\sqrt{2\lambda_2+1}(-)^{J_1+J_3+\lambda_2+\lambda}\begin{Bmatrix}\lambda & \lambda_1 & \lambda_2\\ J_3 & J_2 & J_1\end{Bmatrix}$$
$$\times\sqrt{1+\delta_{n_1n_2}}, \tag{4.2}$$

where $X^{(n_1)}_{J_1J_2}(\lambda_1)$ and $Y^{(n)}_{J_1J_3}(\lambda)$ are the TRPA forward and backward amplitudes, respectively. The scattering matrix elements from one- to two-boson states are

$$\Lambda^{(n)}_{JJ'}(\lambda)=\sum_{J_1,J_2}[X^{(n)}_{J_1J_2}(\lambda)\langle JJ_2|\mathcal{V}|J'J_1\rangle+Y^{(n)}_{J_1J_2}(\lambda)$$
$$\times\langle JJ_1|\mathcal{V}|J'J_2\rangle]. \tag{4.3}$$

It is important to note that the scattering matrix elements change sign depending upon whether the levels j and j' correspond to particle or hole. Therefore, there are big cancellations either for finite or zero temperature. Finally, the spreading width of the GMR is

$$\sigma^2=\sum_{\lambda_1,n_1,\lambda_2,n_2}\{|\langle\lambda n|\mathcal{H}|\lambda_1 n_1,\lambda_2 n_2\rangle|^2$$
$$\times[(n_{\omega_1}+1)(n_{\omega_2}+1)-n_{\omega_1}n_{\omega_2}]$$
$$+|\langle 0|\mathcal{H}|[\lambda_1 n_1,\lambda_2 n_2]_\lambda,\lambda n\rangle|^2$$
$$\times[(n_{\omega_1}+1)(n_{\omega_2}+1)-n_{\omega_1}n_{\omega_2}]\}. \tag{4.4}$$

This final expression for the spreading width considering the changing between $\omega_1\leftrightarrow\omega_2$ is summarized in Fig. 6. It considers all the contributions coming from the NFT diagrams up to the leading order. It depends only on the two-body interaction, the temperature, and the collectivity of the two bosons that mix with the giant resonance.

Making the limit $T\to 0$ in Eq. (4.4), we obtain the spreading width calculated in Ref. [34]. In this limit, the Fermi occupation numbers verify that $(1-n_i)\to 1$ (for particle) and $n_i\to 1$ (for hole), while the Bose occupation-numbers verify that $n_\omega\to 0$, surviving only the particle-hole excitations.

V. ISOSCALAR-ISOVECTOR SEPARABLE INTERACTION

In this paper we discuss the properties of the GMR in the framework of schematic separable forces. In this section we obtain, for normal nucleus at finite temperature, the TRPA solutions of the multipole particle-hole Hamiltonian. We define the single particle ($\mathcal{H}_{sp}$) and the multipole [$\mathcal{H}(\lambda)$]

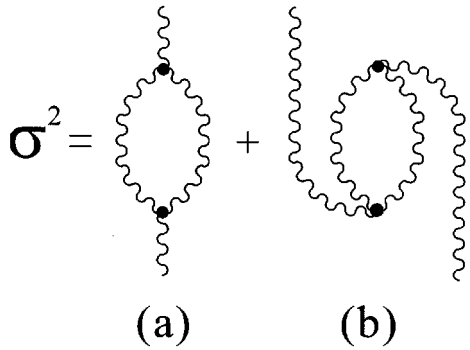

FIG. 6. Schematic representation of the contribution to the square of the spreading width (second moment of the strength function). It must be noted that the two vertices occur at the same τ, which implies that there is no propagator between them. It means that these diagrams have no energy denominators. (a) Contributions from the forward one-boson two-bosons matrix element. (b) Contributions from the backward one-boson two-bosons matrix element. These diagrams are temperature dependent, so the positive and negative TRPA roots in the intermediate two-bosons state must be considered.

Hamiltonians following Refs. [41,36]

$$\mathcal{H}_{\rm sp}=\sum_{J,p}\varepsilon_J a_J^\dagger(p)a_J(p), \tag{5.1}$$

where $p=\nu(\pi)$ labels neutrons (protons), $a_J^\dagger(p)[a_{J_2}(p)]$ are the fermion creation(annihilation) operators, and ε_J are the single-particle energies. The two-body Hamiltonian is

$$\begin{aligned}\mathcal{H}(\lambda)=&-\left(\frac{k_0+k_1+2k'}{2}\right)\sum_\mu \mathcal{Q}^\nu_{\lambda\mu}\mathcal{Q}^{\nu^\dagger}_{\lambda\mu}\\&-\left(\frac{k_0+k_1-2k'}{2}\right)\sum_\mu \mathcal{Q}^\pi_{\lambda\mu}\mathcal{Q}^{\pi^\dagger}_{\lambda\mu}\\&-\left(\frac{k_0-k_1}{2}\right)\sum_\mu [\mathcal{Q}^\pi_{\lambda\mu}\mathcal{Q}^{\nu^\dagger}_{\lambda\mu}+\mathcal{Q}^\nu_{\lambda\mu}\mathcal{Q}^{\pi^\dagger}_{\lambda\mu}],\end{aligned} \tag{5.2}$$

where the quantities k_0, k_1 are the coupling constant of the isoscalar and isovector particle-hole residual interactions, and their relation is obtained from the ratio between the isoscalar and isovector optical potentials [42]. The parameter k' is the coupling constant for the admixture between the isoscalar and isovector modes in the presence of neutron excess. $\mathcal{Q}^\pi_{\lambda\mu}$ and $\mathcal{Q}^\nu_{\lambda\mu}$ are the multipole particle-hole operators built out of neutrons and protons, respectively, and are defined in the following way:

$$\begin{aligned}\mathcal{Q}^p_{\lambda\mu}=&\frac{(-1)}{\hat\lambda}\sum_{J_1\geqslant J_2}\mathcal{M}^p(J_1,J_2;\lambda)[\beta_p^\dagger(J_1,J_2;\lambda\mu)\\&+(-)^{\lambda-\mu}\beta_p(J_1,J_2;\lambda-\mu)],\end{aligned} \tag{5.3}$$

with $\hat\lambda=\sqrt{2\lambda+1}$ and

$$\begin{aligned}\beta_p^\dagger(J_1,J_2;\lambda\mu)=&[a_{J_1}^\dagger(p)a_{J_2}(p)]_{\lambda\mu}\\=&\sum_{m_{J_2},m_{J_1}}\langle J_2J_1m_{J_2}m_{J_1}|\lambda\mu\rangle a^\dagger_{J_2m_{J_2}}\\&\times(p)(-)^{J_1-m_{J_1}}a_{J_1-m_{J_1}}(p),\end{aligned} \tag{5.4}$$

where the index J is used to denote either the state above or below the Fermi surface. The coefficients $\mathcal{M}^p(J_1,J_2;\lambda)$ are defined as

$$\begin{aligned}\mathcal{M}^p(J_1,J_2;\lambda)=&\langle J_1||f^p_\lambda(r)Y_\lambda||J_2\rangle i^{l_{J_2}-l_{J_1}+\lambda}\\=&\mathcal{M}^p(J_2,J_1;\lambda)(-)^{J_1-J_2+\lambda}.\end{aligned} \tag{5.5}$$

We use for the radial dependence of $f^p_\lambda(r)$, peaked around the nuclear surface, $f^p_\lambda(r)=\partial W(r)/\partial r$, where $W(r)$ is a Wood Saxon potential.

The creation operator of a collective excitation is defined in the same way as it is done in the zero-temperature RPA:

$$\begin{aligned}\Gamma^\dagger_{n\lambda\mu}=&\sum_{p,J_1\geqslant J_2}X^{(n)p}_{J_1J_2}\beta_p^\dagger(J_1,J_2;\lambda\mu)\\&-(-)^{\lambda-\mu}Y^{(n)p}_{J_1J_2}\beta_p(J_1,J_2;\lambda-\mu),\end{aligned} \tag{5.6}$$

where this operator (as $\mathcal{Q}^p_{\lambda\mu}$) includes particle-particle ($\varepsilon_{J_1},\varepsilon_{J_2}>\mu$), particle-hole ($\varepsilon_{J_1}>\mu$, $\varepsilon_{J_2}<\mu$), and hole-hole ($\varepsilon_{J_1},\varepsilon_{J_2}<\mu$) excitations. The index n specifies the TRPA root number.

The linearization condition reads

$$\langle[\mathcal{H}_{\rm sp}+\mathcal{H}(\lambda),\Gamma^\dagger_{n\lambda\mu}]\rangle=\hbar\omega_n\Gamma^\dagger_{n\lambda\mu}, \tag{5.7}$$

where $\langle\ \rangle$ denotes the grand canonical ensemble average. This leads to the soscalar-isovector dispersion relation, from where either the ω_n TRPA energies or the isovector and isoscalar strength can be obtained

$$\frac{\Lambda^\pi_n}{\Lambda^\nu_n}=\frac{\hat\lambda^2-(k_0+k_1+2k')\mathcal{F}^\nu_n}{(k_0-k_1)\mathcal{F}^\pi_n}, \tag{5.8}$$

with

$$\mathcal{F}^p_n\Lambda^p_n=\sum_{J_1\geqslant J_2\in p}(n_{J_2}-n_{J_1})\mathcal{M}^p(J_1,J_2;\lambda)[X^{(n)p}_{J_1J_2}+Y^{(n)p}_{J_1J_2}] \tag{5.9}$$

and

$$\begin{aligned}\mathcal{F}^p_n=&\sum_{J_1\geqslant J_2\in p}(n_{J_2}-n_{J_1})\mathcal{M}^p(J_1,J_2;\lambda)^2\\&\times\left[\frac{1}{\varepsilon^p_{J_1J_2}-\hbar\omega}{}_n+\frac{1}{\varepsilon^p_{J_1J_2}+\hbar\omega_n}\right].\end{aligned} \tag{5.10}$$

The amplitudes that define the TRPA bosons are given by

$$X^{(n)p}_{J_1J_2}=\frac{\Lambda^p_n\mathcal{M}^p(J_1,J_2;\lambda)}{\varepsilon^p_{J_1J_2}-\hbar\omega_n},\quad Y^{(n)p}_{J_1J_2}=\frac{\Lambda^p_n\mathcal{M}^p(J_1,J_2;\lambda)}{\varepsilon^p_{J_1J_2}+\hbar\omega_n}. \tag{5.11}$$

The particle-vibration coupling strength, Λ^p_n, is determined through Eq. (5.8) and the normalization condition of the TRPA bosons

$$\begin{aligned}(\Lambda^\nu_n)^{-2}=&\sum_{j_1\geqslant j_2\in\nu}(n_{j_2}-n_{j_1})\mathcal{M}^\nu(j_1,J_2;\lambda)^2\frac{4\varepsilon^\nu_{j_1j_2}\hbar\omega_n}{(\varepsilon^\nu_{j_1j_2})^2-(\hbar\omega_n)^2}\\&+\sum_{j_1\geqslant j_2\in\pi}\left[\frac{\hat\lambda^2-(k_0+k_1+2k')\mathcal{F}^\nu_n}{(k_0-k_1)\mathcal{F}^\pi_n}\right]^2\\&\times(n_{j_2}-n_{j_1})\mathcal{M}^\pi(j_1,j_2;\lambda)^2\frac{4\varepsilon^\pi_{j_1j_2}\hbar\omega_n}{(\varepsilon^\pi_{j_1j_2})^2-(\hbar\omega_n)^2}.\end{aligned} \tag{5.12}$$

VI. RESULTS

In the present section we apply our model to the giant dipole resonance (GDR). We have calculated the spreading width of the GDR 1^- in the ^{208}Pb and ^{90}Zr isotopes. The TRPA roots are obtained using a isoscalar-isovector separable interaction, developed in the previous section. For the radial dependence of the interaction, peaked around the

nuclear surface, we use the $\partial \mathcal{V}(r)/\partial r$, with $\mathcal{V}(r)$ the Woods-Saxon potential

$$\mathcal{V}(r)=\frac{-V_0}{\left[1+\exp\left(\frac{r-R_0}{a}\right)\right]}, \tag{6.1}$$

with

$$V_0=50 \text{ MeV}, \quad R_0=r_0A^{1/3}, \quad a=0.5 \text{ fm}, \quad r_0=1.2 \text{ fm}. \tag{6.2}$$

The set of single-particle levels was obtained using the spherical harmonic oscillator levels with the corrections due to the centrifugal and spin-orbit interactions [43]

$$\frac{E}{\hbar\omega}=N+\frac{3}{2}-\kappa l-\mu\left(l(l+1)-\frac{N(N+3)}{2}\right) \quad \text{for } j=l+1/2$$

$$\frac{E}{\hbar\omega}=N+\frac{3}{2}-\kappa(l+1)-\mu\left(l(l+1)-\frac{N(N+3)}{2}\right) \quad \text{for } j=l-1/2, \tag{6.3}$$

where $\hbar\omega=41\,A^{-1/3}$ with A the mass number of the nucleus, and N,j,l are the principal quantum number and the total and orbital angular momentum quantum numbers, respectively. κ and μ are chosen to obtain the best fit for each nucleus [44].

We have defined the single-particle levels starting from $N=0$ up to 3 shells over the Fermi level. These are good enough for our calculations only for the levels around the Fermi surface, where we use the neighboring odd isotope data of the ^{208}Pb and ^{90}Zr. The change of the single-particle energies around the Fermi surface has been done, in both cases, taking care of keeping the energy-baricenter of the exchanged levels in the same position. Thermal Hartree-Fock calculations [45] have shown that the single-particle energies have weak temperature dependence. Therefore, we use the zero temperature energies and wave functions all over our calculations.

The isoscalar strength k_0 is determined by fixing the energy of the first collective TRPA root. The isovector strength k_1 and the coupling constant of the two modes are determined using the following formulas [41,36]:

TABLE I. Temperature dependence of the GDR energy and the proton and neutron chemical potentials, for the ^{208}Pb. The GDR energy, chemical potentials, and temperature are given in MeV.

	$T=1$	$T=2$	$T=3$	$T=4$	$T=5$
$\omega_{\rm GDR}$	14.06	13.85	13.63	13.41	13.22
μ_n	−0.37	−0.64	−1.01	−1.50	−2.10
μ_p	−0.30	−0.55	−0.97	−1.54	−2.27

$$\frac{k_0}{k_1}=0.21(3+2\lambda)\frac{V_1}{V_0},$$

$$k'=-\frac{1}{2}k_1\frac{N-Z}{A}, \tag{6.4}$$

where $V_1=120$ MeV and $V_0=-50$ MeV are the depth of the isovector and isoscalar potentials, respectively. N, Z, and A are the neutron, proton, and mass numbers of the corresponding nucleus.

For the calculation of the spreading width of the GDR 1^- in the ^{208} Pb and ^{90} Zr we use, as intermediate bosons, all the TRPA roots (collective and noncollective ones) with excitation energies $\omega_n \leqslant 30$ MeV and multipolarities $\lambda=0,1,2,3,4,5$.

The ratio of the isoscalar-isovector strength of the separable interaction is checked using the energy of the available experimental data, for the adiabatic and giant roots at zero temperature, for all the multipolarities, verifying quite well the relations of Eq. (6.4).

The chemical potential μ_p is adjusted for each temperature in such a way that the particle number average is conserved:

$$\langle N\rangle=\sum_{j_\nu\in\nu} n_{j_\nu}, \quad \langle P\rangle=\sum_{j_\pi\in\pi} n_{j_\pi}. \tag{6.5}$$

In Table I (Table III) we show the variation with the temperature of the GDR energy and the proton and neutron chemical potentials for ^{208}Pb (^{90}Zr). In Table II (Table IV) are shown, for the ^{208}Pb (^{90}Zr), the temperature dependence of the partial contributions to the square of the spreading width σ^2. These contributions correspond to the sum of all the TRPA roots for a given angular momentum of the intermediate-boson states of the diagrams of Fig. 6 [see Eq. (4.4)].

TABLE II. Relative contribution [Eq. (4.4)] to the square of the spreading width σ^2 of the diagrams of Fig. 6 for the ^{208}Pb. B_1 is the contribution of Fig. 6(a) and B_2 of Fig. 6(b), both of them including the change between $\lambda_1\leftrightarrow\lambda_2$, λ_1 and λ_2 being the quantum numbers of the intermediate boson states.

Int. Bosons	$T=1$		$T=2$		$T=3$		$T=4$		$T=5$	
$\lambda_1^\pi\ \lambda_2^\pi$	B_1	B_2	B_1	B_2	B_1	B_2	B_1	B_2	B_1	B_2
1^-0^+	0.43	0.06	0.37	0.04	0.32	0.03	0.31	0.03	0.31	0.03
2^+1^-	3.18	0.58	3.19	0.66	3.06	0.63	3.14	0.61	3.24	0.57
3^-2^+	5.12	1.08	6.00	1.48	6.68	1.60	7.08	1.72	9.23	1.71
4^+3^-	5.65	1.35	6.70	2.09	7.71	2.31	9.32	2.36	11.48	2.31
5^-4^+	5.92	0.90	6.09	0.99	6.59	0.97	8.02	1.00	10.85	1.04

TABLE III. Temperature dependence of the GDR energy and the proton and neutron chemical potentials for the ^{90}Zr. The GDR energy, chemical potentials, and temperature are given in MeV.

	$T=1$	$T=2$	$T=3$	$T=4$	$T=5$
ω_{GDR}	16.70	16.63	16.54	16.48	16.39
μ_n	−1.56	−2.15	−2.76	−3.73	−4.05
μ_p	−1.22	−1.48	−1.92	−2.51	−3.22

The final results of the calculation of the GDR spreading width 1^-, for the ^{208}Pb and ^{90}Zr isotopes, are shown in Fig. 7 and Fig. 8, respectively.

VII. CONCLUSIONS

Most of the approaches to evaluate the spreading width consider that σ is produced by the admixture between the GMR and more complicated structures, mainly two-particle–two-hole states. If the ground state correlations are considered through an RPA or TRPA treatment of the collective states, the problem gets more complicated. In Ref. [34] we have developed a method that considers all the contributions to the spreading width of the GMR, corresponding to the leading order in the NFT perturbation theory.

In this paper, we extended the calculation of the spreading width at finite temperature, using the short time discontinuity of the second derivative of the collective Green's function. We extend the method of Ref. [37] to temperature dependent propagators, which introduce temperature dependent probabilities for both fermionic and bosonic states. In this way, we can define an effective interaction vertex between one-boson and two-bosons of the TRPA that simplify greatly the calculation. The ground state fluctuations are considered through the so-called backward vertex [see Fig. 5(b)].

It has been suggested [46] that there exist two main factors that produce the strong increase of the spreading width with the temperature, the fluctuations of the nuclear surface, and the transfer angular momentum, but neither factor is enough to explain the experimental data, mainly in the region of medium and high temperatures. Therefore, we consider it of interest to see if the spreading width of the GMR increases continuously with the temperature [33] or saturates at a certain temperature [32]. Our model is based in the same physical concepts as Ref. [32], but our method of working in a complete basis of collective TRPA states, instead of using an overcomplete basis of bosons and particle-holes, yields a factorization of the result that reduced drastically the number of diagrams to calculate. This method ensures that all the contributions at leading order are considered, without any approximation neither over the temperature occupation probabilities nor over the diagrams involved. It would be also possible to solve the TRPA in the continuum using Gamow resonances [22,24] in order to consider both together, the spreading and the escaping width of the resonance.

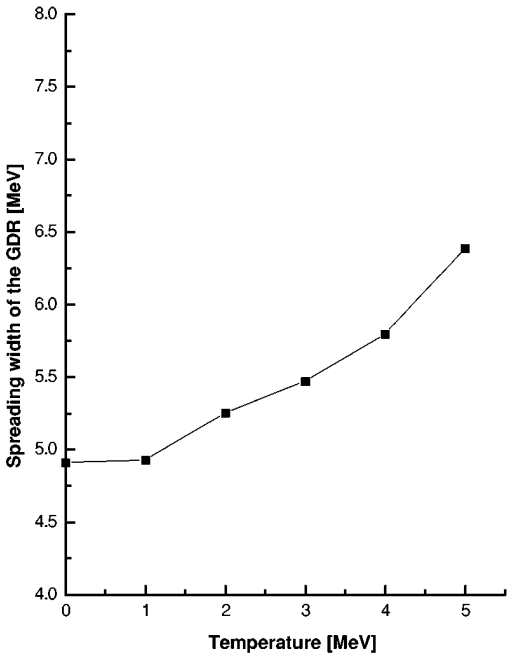

FIG. 7. Spreading width of the giant dipole resonance (1^-) of ^{208}Pb as a function of the temperature, given by Eq. (4.4).

We have considered a modelistic isovector-isoscalar separable interaction that includes most of the physical properties of interest. We observed that the spreading width increases with the temperature, as was pointed out in Ref. [33], without saturation until 5 MeV (see Fig. 7 and Fig. 8). We do not discard a possible saturation at higher temperatures.

Another important aspect of this work was related to the study of the temporal permutations of the diagrams contributing to the self-energy. We observed that it is possible to reconstruct the finite temperature results inserting the corresponding occupation factors in the zero-temperature expression. For each fermion (boson) in the diagrams at zero temperature, one has to add only the occupation number of the fermion (boson) to obtain the corresponding diagrams at finite temperature. Additionally, the negative TRPA solutions

TABLE IV. Relative contribution [Eq. (4.4)] to the square of the spreading width σ^2 of the diagrams of Fig. 6 for the ^{90}Zr. B_1 is the contribution of Fig. 6(a) and B_2 of Fig. 6(b), both of them including the change between $\lambda_1 \leftrightarrow \lambda_2$, where λ_1 and λ_2 are the quantum numbers of the intermediate boson states.

Int. Bosons	$T=1$		$T=2$		$T=3$		$T=4$		$T=5$	
$\lambda_1^{\pi}\lambda_2^{\pi}$	B_1	B_2	B_1	B_2	B_1	B_2	B_1	B_2	B_1	B_2
1^-0^+	1.02	0.17	0.96	0.11	0.96	0.09	1.05	0.07	1.03	0.56
2^+1^-	2.53	1.10	3.37	2.16	4.27	3.12	6.37	3.66	6.78	2.71
3^-2^+	2.51	1.09	3.60	2.48	5.13	3.36	8.72	5.20	9.54	4.72
4^+3^-	4.82	0.93	4.48	0.75	4.56	0.65	4.93	0.51	6.11	0.49
5^-4^+	9.29	3.22	8.76	2.89	8.99	2.50	9.45	1.67	14.04	1.98

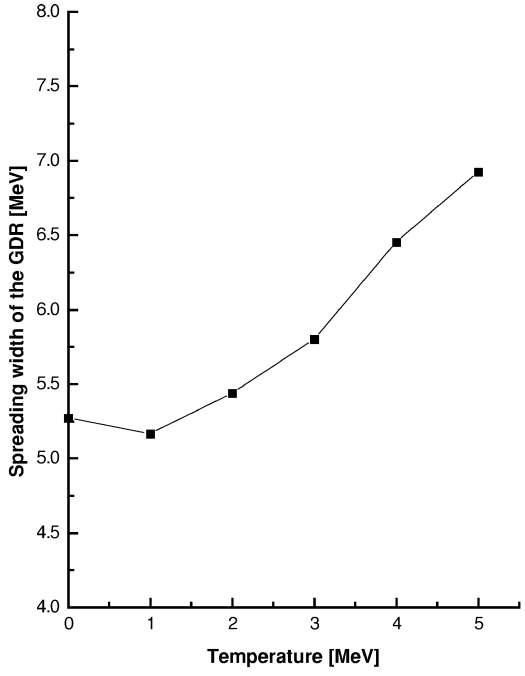

FIG. 8. Spreading width of the giant dipole resonance 1^- of ^{90}Zr as a function of the temperature, given by Eq. (4.4).

must be included to consider all the contributions to the spreading width.

APPENDIX A

In this appendix we show that the Bose and Fermi occupation numbers could be factorized if one can sum conveniently the relevant diagrams contributing to the spreading width.

We consider the case in which there are not two equal fermionic states. Therefore, one has to consider the contributions to the self-energy from the diagrams that have two triangles [Fig. 4(c), 4(d), 4(e), 4(f)]. We will choose, as an example, the different τ permutations of Figs. 4(c), 4(d), 4(e), 4(f) that have the following Fermi occupation numbers, $n_{J_1}n_{J_2}(1-n_{J_3})n_{J_4}n_{J_5}(1-n_{J_6})$ independently of the Bose occupation numbers. We will also take into account the τ permutations with the opposite occupation numbers, i.e., all the diagrams that can be obtained changing $[(1-n_i)\leftrightarrow n_i,\ (1+n_\omega)\leftrightarrow n_\omega]$.

There is no τ permutation of Fig. 4(c) with these Fermi occupation numbers. Three τ permutations of Fig. 4(d) have these Fermi occupation numbers. Following the rules given in Sec. III, the sum of the contributions to the self-energy is equal to

$$\frac{1}{\beta}\sum_{k_n=par} e^{-ik_n(\tau''-\tau')} \sum_{J_1J_2J_3J_4J_5J_6,\lambda_1} \mathcal{V}(J_1,J_3;GR)\mathcal{V}(J_6,J_5;GR)\mathcal{V}(J_2,J_3,J_4,J_5)\mathcal{V}(J_1,J_2;\lambda_1)\mathcal{V}(J_4,J_6;\lambda_1)$$

$$\times\left\{\frac{[n_{J_1}n_{J_2}(1-n_{J_3})n_{J_4}n_{J_5}(1-n_{J_6})n_{\omega_1}+(1-n_{J_1})(1-n_{J_2})n_{J_3}(1-n_{J_4})(1-n_{J_5})n_{J_6}(1+n_{\omega_1})]}{(ik_n-\tilde{\varepsilon}_{65})(ik_n-\tilde{\varepsilon}_{13})(ik_n-\tilde{\varepsilon}_{23}-\omega_1)(\tilde{\varepsilon}_{46}+\omega_1)}\right.$$

$$\left.+\frac{[n_{J_1}n_{J_2}(1-n_{J_3})n_{J_4}n_{J_5}(1-n_{J_6})(1+n_{\omega_1})+(1-n_{J_1})(1-n_{J_2})n_{J_3}(1-n_{J_4})(1-n_{J_5})n_{J_6}n_{\omega_1}]}{(ik_n-\tilde{\varepsilon}_{65})(ik_n-\tilde{\varepsilon}_{13})(ik_n-\tilde{\varepsilon}_{23}+\omega_1)(\tilde{\varepsilon}_{46}-\omega_1)}\right\}, \tag{A1}$$

where GR labels the giant resonance TRPA root. The sum over λ_1 implies a sum over all the possible multipolarities of the complete collective basis of TRPA roots.

Three τ permutations of the Fig. 4(e) have also these Fermi occupation numbers, the sum of them being equal to

$$\frac{1}{\beta}\sum_{k_n=even} e^{-ik_n(\tau''-\tau')} \sum_{J_1,J_2,J_3,J_4,J_5,J_6,\lambda_2} \mathcal{V}(J_1,J_3;GR)\mathcal{V}(J_6,J_5;GR)\mathcal{V}(J_1,J_2,J_4,J_6)\mathcal{V}(J_2,J_3;\lambda_2)\mathcal{V}(J_4,J_5;\lambda_2)$$

$$\times\left\{\frac{[n_{J_1}n_{J_2}(1-n_{J_3})n_{J_4}n_{J_5}(1-n_{J_6})(1+n_{\omega_2})+(1-n_{J_1})(1-n_{J_2})n_{J_3}(1-n_{J_4})(1-n_{J_5})n_{J_6}n_{\omega_2}]}{(ik_n-\tilde{\varepsilon}_{65})(ik_n-\tilde{\varepsilon}_{13})(ik_n-\tilde{\varepsilon}_{64}-\omega_2)(\tilde{\varepsilon}_{32}+\omega_2)}\right.$$

$$\left.+\frac{[n_{J_1}n_{J_2}(1-n_{J_3})n_{J_4}n_{J_5}(1-n_{J_6})n_{\omega_2}+(1-n_{J_1})(1-n_{J_2})n_{J_3}(1-n_{J_4})(1-n_{J_5})n_{J_6}(1+n_{\omega_2})]}{(ik_n-\tilde{\varepsilon}_{65})(ik_n-\tilde{\varepsilon}_{13})(ik_n-\tilde{\varepsilon}_{64}+\omega_2)(\tilde{\varepsilon}_{32}-\omega_2)}\right\}. \tag{A2}$$

Twenty τ permutations of Fig. 4(f) contribute with the same Fermi occupation probabilities. The sum of all of them are equal to

$$\frac{1}{\beta}\sum_{k_n=even} e^{-ik_n(\tau''-\tau')} \sum_{J_1,J_2,J_3,J_4,J_5,J_6,\lambda_1,\lambda_2} \mathcal{V}(J_1,J_3;GR)\mathcal{V}(J_6,J_5,GR)\mathcal{V}(J_1,J_2;\lambda_1)\mathcal{V}(J_4,J_6;\lambda_1)\mathcal{V}(J_2,J_3;\lambda_2)\mathcal{V}(J_4,J_5;\lambda_2)$$

$$\times\frac{1}{(ik_n-\widetilde{\varepsilon}_{65})(ik_n-\widetilde{\varepsilon}_{13})(ik_n-\omega_1-\omega_2)}$$

$$\times\left\{\frac{n_{J_1}n_{J_2}(1-n_{J_3})n_{J_4}n_{J_5}(1-n_{J_6})(1+n_{\omega_2})+(1-n_{J_1})(1-n_{J_2})n_{J_3}(1-n_{J_4})(1-n_{J_5})n_{J_6}n_{\omega_2}}{(ik_n-\widetilde{\varepsilon}_{64}-\omega_2)(\widetilde{\varepsilon}_{32}+\omega_2)}\right.$$

$$\left.+\frac{n_{J_1}n_{J_2}(1-n_{J_3})n_{J_4}n_{J_5}(1-n_{J_6})n_{\omega_1}+(1-n_{J_1})(1-n_{J_2})n_{J_3}(1-n_{J_4})(1-n_{J_5})n_{J_6}(1+n_{\omega_1})}{(ik_n-\widetilde{\varepsilon}_{23}-\omega_1)(\widetilde{\varepsilon}_{46}+\omega_1)}\right\}$$

$$-\{\text{same as above with } \omega_1\rightarrow-\omega_1\}-\{\text{same as above with } \omega_2\rightarrow-\omega_2\}$$

$$+\{\text{same as above with } \omega_1\rightarrow-\omega_1 \text{ and } \omega_2\rightarrow-\omega_2\}. \tag{A3}$$

One way to factorize conveniently the different τ permutation is using the property that verifies the TRPA solutions for separable interactions (see Appendix B). This expression relates the fermionic two-body interaction with the TRPA fermion-boson matrix elements, and is given by

$$\mathcal{V}(i,j,k,l)=-\sum_n \mathcal{V}(i,j;\lambda_n)\mathcal{V}(k,l;\lambda_n)\left[\frac{1}{\widetilde{\varepsilon}_{ij}-\omega_n}-\frac{1}{\widetilde{\varepsilon}_{ij}+\omega_n}\right], \tag{A4}$$

where the sum is over all the TRPA roots with multipolarity λ, and is valid for any particle-hole state i,j.

Replacing the corresponding fermionic matrix element in the Eq. (A1) and Eq. (A2), and summing for all the τ permutations, we arrive to the result

$$\frac{1}{\beta}\sum_{k_n=even} e^{-ik_n(\tau''-\tau')} \sum_{J_1,J_2,J_3,J_4,J_5,J_6,\lambda_1,\lambda_2} \frac{[(1+n_{\omega_1})(1+n_{\omega_2})-n_{\omega_1}n_{\omega_2}]}{(ik_n-\omega_1-\omega_2)}\frac{\mathcal{V}(J_4,J_5;\lambda_2)\mathcal{V}(J_6J_5,GR)\mathcal{V}(J_4,J_6;\lambda_1)}{(ik_n-\widetilde{\varepsilon}_{65})(\widetilde{\varepsilon}_{64}-\omega_1)}$$

$$\times\frac{\mathcal{V}(J_1,J_3;GR)\mathcal{V}(J_1,J_2;\lambda_1)\mathcal{V}(J_2,J_3;\lambda_2)}{(\widetilde{\varepsilon}_{23}-\omega_2)(ik_n-\widetilde{\varepsilon}_{13})}[(1-n_{J_1})(1-n_{J_2})n_{J_3}(1-n_{J_4})(1-n_{J_5})n_{J_6}+n_{J_1}n_{J_2}(1-n_{J_3})n_{J_4}n_{J_5}(1-n_{J_6})]$$

$$-\{\text{same as above with } \omega_1\rightarrow-\omega_1\}-\{\text{same as above with } \omega_2\rightarrow-\omega_2\}$$

$$+\{\text{same as above with } \omega_1\rightarrow-\omega_1 \quad \text{and} \quad \omega_2\rightarrow-\omega_2\}. \tag{A5}$$

In this expression are factorized the Bose and the Fermi occupation numbers.

If we make a similar analysis, for the reverse circulation of the triangle, and we sum it up with the Eq. (A5) we obtain

$$\frac{1}{\beta}\sum_{k_n=even} e^{-ik_n(\tau''-\tau')} \sum_{J_1,J_2,J_3,J_4,J_5,J_6,\lambda_1,\lambda_2} \frac{[(1+n_{\omega_1})(1+n_{\omega_2})-n_{\omega_1}n_{\omega_2}]}{(ik_n-\omega_1-\omega_2)}[n_{J_1}n_{J_2}(1-n_{J_3})-(1-n_{J_1})(1-n_{J_2})n_{J_3}]$$

$$\times\frac{\mathcal{V}(J_1,J_3;GR)\mathcal{V}(J_1,J_2;\lambda_1)\mathcal{V}(J_2,J_3;\lambda_2)}{(\widetilde{\varepsilon}_{23}-\omega_2)(ik_n-\widetilde{\varepsilon}_{13})}[n_{J_4}n_{J_5}(1-n_{J_6})-(1-n_{J_4})(1-n_{J_5})n_{J_6}]$$

$$\times\frac{\mathcal{V}(J_4,J_5;\lambda_2)\mathcal{V}(J_6,J_5,GR)\mathcal{V}(J_4,J_6;\lambda_1)}{(ik_n-\widetilde{\varepsilon}_{65})(\widetilde{\varepsilon}_{64}-\omega_1)}-\{\text{same as above with } \omega_1\rightarrow-\omega_1\}-\{\text{same as above with } \omega_2\rightarrow-\omega_2\}$$

$$+\{\text{same as above with } \omega_1\rightarrow-\omega_1 \quad \text{and} \quad \omega_2\rightarrow-\omega_2\}, \tag{A6}$$

where, in this expression, three well-differentiated factors can be seen. The first is related to the two intermediate boson

propagators and depends on the energy and occupation numbers of these bosons. The other two factors represent the matrix element between one-boson and two-boson states and depend on the Fermi occupation numbers of the triangles, the boson-fermion interaction, and the particle-hole amplitudes in the TRPA collective states.

APPENDIX B

The TRPA solutions verify the following rule when a separable isoscalar-isovector interaction is used. Expanding the matrix element of any particle-hole operator between a particle-hole state and the ground state in terms of the strength distribution over the TRPA bosons, we arrive at

$$\sum_n \mathcal{F}_n^{\rho}\Lambda_n^{\rho}\left[\frac{\Lambda_n^{\rho_1}\mathcal{M}^{\rho_1}(J_1,J_2,\lambda)}{\varepsilon_{J_1J_2}^{\rho_1}-\hbar\omega_n}-\frac{\Lambda_n^{\rho_1}\mathcal{M}^{\rho_1}(\alpha_1,J_2,\lambda)}{\varepsilon_{J_1J_2}^{\rho_1}+\hbar\omega_n}\right]=\mathcal{M}^{\rho}(J_1,J_2,\lambda)\,\delta_{\rho_1 p}, \tag{B1}$$

where the sum is over all the TRPA roots n and ρ,ρ_1 label neutron or proton states. This expression is valid for any particle-hole state J_1,J_2 for either proton or neutrons. Looking at the dispersion relation [Eq. (5.8)], and replacing in the equation above, we obtain

$$\begin{aligned}
\sum_n \Lambda_n^{\nu^2}\left[\frac{1}{\varepsilon_{J_1J_2}^{\nu}-\hbar\omega_n}-\frac{1}{\varepsilon_{J_1J_2}^{\nu}+\hbar\omega_n}\right]&=\frac{(k_0+k_1+2k')}{\hat{\lambda}^2},\\
\sum_n \Lambda_n^{\pi^2}\left[\frac{1}{\varepsilon_{J_1J_2}^{\pi}-\hbar\omega_n}-\frac{1}{\varepsilon_{J_1J_2}^{\pi}+\hbar\omega_n}\right]&=\frac{(k_0+k_1-2k')}{\hat{\lambda}^2},\\
\sum_n \Lambda_n^{p}\Lambda_n^{p_1}\left[\frac{1}{\varepsilon_{J_1J_2}^{p}-\hbar\omega_n}-c1\,\varepsilon_{J_1J_2}^{p}+\hbar\omega_n\right]&=\frac{(k_0-k_1)}{\hat{\lambda}^2}.
\end{aligned} \tag{B2}$$

These Equations could also be useful for checking the TRPA results.

[1] K. Snover, Annu. Rev. Nucl. Part. Sci. **36**, 545 (1986).
[2] E. Suraud, Ch. Gregoire, and B. Tamain, Prog. Part. Nucl. Phys. **23**, 357 (1989).
[3] E. Ramakrishnan *et al.*, Nucl. Phys. **A599**, 49c (1996).
[4] P. Piatelli *et al.*, Nucl. Phys. **A599**, 63c (1996).
[5] A. Bracco, F. Camera, M. Mattiuzzi, d. Gnaccolini, B. Million, J. J. Gaardhøje, A. Maj, and T. Tveter, Nucl. Phys. **A599**, 83c (1996).
[6] M. Cinausero *et al.* Nucl. Phys. **A599**, 111c (1996).
[7] H. M. Sommermann, Ann. Phys. (N.Y.) **151**, 163 (1983).
[8] A. L. Goodman, Nucl. Phys. **A352**, 30 (1981); **A352**, 45 (1981).
[9] A. L. Goodman, Phys. Rev. C **35**, 2338 (1987).
[10] J. L. Egido and P. Ring, J. Phys. G **19**, 1 (1993).
[11] W. E. Ormand, P. F. Bortignon, and R. A. Broglia, Nucl. Phys. **A599**, 57c (1996).
[12] P. Donati, N. Giovanardi, P. F. Bortignon, and R. A. Broglia, Phys. Lett. B **383**, 15 (1996).
[13] D. R. Chakrabarty, S. Sen, N. Alamanos, P. Paul, R. Schicker, J. Stachel, and J. J. Gaardhøje, Phys. Rev. C **36**, 1886 (1987).
[14] A. Bracco, J. J. Gaardhøje, A. M. Bruce, J. D. Garrett, B. Herskind, M. Pignanelli, D. Barneoud, H. Nifenecker, J. A. Pinston, C. Ristori, F. Schussler, J. Bacelar, and H. Hofmann, Phys. Rev. Lett. **62**, 2080 (1989).
[15] P. F. Bortignon, A. Bracco, D. Brink, and R. A. Broglia, Phys. Rev. Lett. **67**, 3360 (1991).
[16] K. Yoshida, J. Kasagi, H. Hama, M. Sakurai, M. Kodama, K. Furutaka, K. Ieki, W. Galster, T. Kubo, and M. Ishihara, Phys. Lett. B **245**, 7 (1990).
[17] J. J. Gaardhøje, A. M. Bruce, and B. Herskind, Nucl. Phys. **A482**, 121 (1988).
[18] R. A. Broglia, T. Døssing, B. Lauritzen, and B. R. Mottelson, Phys. Rev. Lett. **58**, 326 (1987).
[19] B. Lauritzen, R. A. Broglia, W. E. Ormand, and T. Døssing, Phys. Lett. B **207**, 238 (1988).
[20] M. Gallardo, M. Diebel, T. Døssing, and R. A. Broglia, Nucl. Phys. **A443**, 415 (1985).
[21] G. G. Dussel, H. Fortunato, and H. M. Sofia, Phys. Rev. C **42**, 2093 (1990).
[22] P. Curutchet, T. Vertse, and R. J. Liotta, Phys. Rev. C **39**, 1020 (1989).
[23] E. Maglione, R. J. Liotta, and T. Vertse, Phys. Lett. B **298**, 1 (1993).
[24] T. Vertse, P. Curutchet, and R. J. Liotta, Phys. Rev. C **42**, 2605 (1990).
[25] R. J. Liotta, E. Maglione, and T. Vertse, Nucl. Phys. **A599**, 327c (1996).
[26] H. Sagawa and G. F. Bertsch, Phys. Lett. **146B**, 138 (1984).
[27] G. F. Bertsch, P. F. Bortignon, and R. A. Broglia, Rev. Mod. Phys. **55**, 287 (1983).
[28] P. F. Bortignon and R. A. Broglia, Nucl. Phys. **A371**, 405 (1981).

[29] B. Schwesinger and J. Wambach, Phys. Lett. **134B**, 29 (1984).
[30] J. Sawicki, Nucl. Phys. **23**, 285 (1961).
[31] V. G. Soloviev, C. Stoyanov, and A. I. Vdovin, Nucl. Phys. **A288**, 376 (1977).
[32] P. F. Bortignon, R. A. Broglia, G. F. Bertsch, and J. Pacheco, Nucl. Phys. **A460**, 149 (1986).
[33] C. Yanhuang and M. Di Toro, Phys. Rev. C **39**, 105 (1989).
[34] G. G. Dussel, E. C. Seva, and H. M. Sofia, Phys. Rev. C **49**, 1989 (1994).
[35] D. R. Bes, G. G. Dussel, R. A. Broglia, R. J. Liotta, and B. R. Mottelson, Phys. Lett. **52B**, 253 (1974); D. R. Bes, R. A. Broglia, G. G. Dussel, R. J. Liotta, and H. M. Sofia, Nucl. Phys. **A260**, 1 (1976); **A260**, 27 (1976); **A260**, 77 (1976).
[36] P. F. Bortignon, R. A. Broglia, D. R. Bes, and R. J. Liotta, Phys. Rep., Phys. Lett. **30C**, 307 (1977).
[37] M. Baranger, Nucl. Phys. **A149**, 225 (1970).
[38] A. A. Abrikosov, L. P. Gorkov and I. E. Dzyaloshinski, *Methods of Quantum Field Theory in Statistical Mechanics* (Prentice Hall, New Jersey, 1963).
[39] A. L. Fetter and J. D. Walecka, *Quantum Theory of Many Particle System* (McGraw-Hill, Inc., New York 1971).
[40] G. D. Mahan, *Many Particle Physics* (Plenum, New York, 1981).
[41] D. R. Bes, R. A. Broglia, and B. Nilsson, Phys. Rep., Phys. Lett. **16C**, 1 (1975).
[42] A. Bohr and B. R. Mottelson, *Nuclear Structure*, Vol. I (Benjamin, New York, 1969); Vol. II (1975).
[43] S. G. Nilsson, C. F. Tsang, A. Sobiczewski, Z. Szymanski, S. Wycech, C. Gustafson, I. L. Lamm, P. Moller, and B. Nilsson, Nucl. Phys. **A131**, 1 (1969).
[44] C. Dasso (private communication).
[45] P. Bonche, S. Levit, and D. Vautherin, Nucl. Phys. **A427**, 278 (1984).
[46] P. F. Bortignon, A. Bracco, F. De Blasio, E. Ormand, and R. A. Broglia, Nucl. Phys. **A553**, 501 (1993).